Mechanical and Microstructural Evaluation of Laser Assisted Cold Sprayed Bio-ceramic Coatings: Potential Use for Biomedical Applications

Monnamme Tlotleng[1, 2*], Esther Akinlabi[2], Mukul Shukla[3,4] and Sisa Pityana[1, 5]

[1]Council for Scientific and Industrial Research, National Laser Center, Laser Material Processing, Pretoria, 0001, South Africa. [2]University of Johannesburg, Department of Mechanical Engineering Science, Auckland Park, Kingsway Campus, Johannesburg, 2006, South Africa. [3]University of Johannesburg, Department of Mechanical Engineering Technology, Doornfontein Campus, Johannesburg, 2006, South Africa, [4]Department of Mechanical Engineering, MNNIT, Allahabad UP, 211004, India. [5] Department of Chemical and Metallurgical Engineering, Tshwane University of Technology, Pretoria, 0001, South Africa.

*Corresponding authors:MTlotleng@csir.co.za

Abstract

Coatings of commercial pure titanium (CP)-Ti and HAP bio-ceramic were synthesised on Ti-6Al-4V substrate using laser assisted cold spray (LACS) deposition technique. The LACS system comprised of 4.4 kW Nd:YAG laser system, AT-12000HPHV 5000PSI (35 bar) powder feeder (Thermach Inc., Appleton), a De Laval supersonic nozzle and a highly compressed nitrogen gas system. For deposition, the bio-ceramic powder composition, now named 20 wt. %, HAP and 80 wt. %, HAP, was varied while the laser power, the N_2 gas pressure, powder feed rate and the scanning speed were kept at constant. The achieved coatings, at laser power of 2.5 kW, were analysed for the microstructures, mechanical-hardness, composition and bio-corrosion using available analytical techniques. The optical microscope results indicated that the bio-ceramic coatings were most porous when compared to the (CP)-Ti coating. The XRD concluded that the ceramic coatings had no deleterious phase material such as CaO which typically cause delamination during service. The hardness values for the bio-ceramic coatings were high than that of the (CP)-Ti coating. At the interface, the hardness values were low for the 80 wt. %, HAP followed by the 20 wt. %, HAP then CP-Ti. This could mean that the ceramic coatings are ductile. The bonding is attributed to the entrapment of HAP by the molten Ti during rapid heating/ cooling at the substrate. Similarly, the bio-corrosion test indicated that the ceramic coating is highly active in the Hank's solution when compared to the (CP)-Ti coating.

1.0. INTRODUCTION

Metals and their alloys can be used in tissue engineering as permanent or temporary scaffolds. Metals such as stainless steel (SS) have good mechanical properties (stiffness, elasticity and ductility) that are necessary for the fabrication of long bone and screws, but they are prone to corrosion and non-biocompatible. For this understanding, SS scaffolds are preferred only as temporary implants while cobalt alloys (CoCrMo) are favourable for orthopaedics since they are good electrical conducting materials and have better corrosion and fatigue resistant properties. Unfortunately, CoCrMo have stiffness greater than that of SS and titanium alloy (Ti-6Al-4V), hence they have not been used successfully for the long bone replacement applications. [1-3] Titanium alloys are bio-inert, have excellent biocompatibility; low cyto-toxic reaction and good elasticity properties, but lack osteo-conductivity.[4-5] To date, Ti-6Al-4V is the most preferred material over other metal alloys for the orthopaedic applications.[3-5] The low-cyto toxicity reported with Ti-6Al-4V is triggered by the leaching of V ions into the human fluid system after the long service of the implants.[6] The V ions normally lead to disease such as Alzheimer's, neuropathy and Ostemomalacia.[3] It is proposed that to remove this post implantation disease and induce the osseointegration of Ti-6Al-4V, their surface properties must be altered by coating with hydroxyapatite.

Hydroxyapatite (HAP), the most researched bio ceramic material for tissue engineering applications, is brittle; heat sensitive, ductile and porous in nature. Due to its brittleness, HAP cannot be used as a bulk material for structural support[8], except as a compressive material where it can be able to suppress V ions, while accelerate the attachment and growth of the human natural tissue into the metal scaffolds. The porous nature of HAP make it possible that after Osseo-integration nutrition can flow within the scaffolds.[7, 9, 10] Traditionally, HAP has been surface coated on Ti-6Al-4V with wet techniques such as cathodic deposition, Sol-gel, magnetron sputtering, pulse laser deposition and seeded hydrothermal deposition. In addition, thermal and plasma spray techniques have been used. To date the most preferred method of coating HAP is plasma spraying. Recently, cold deposition techniques have emerged given the shortcomings presented with plasma and wet deposition techniques respectively. Disadvantages and advantages of these coating techniques are presented and discussed in details by Doronzhkin.[7]

In summary, it is explained that wet deposition techniques cannot achieve thick, continuous HAP coatings while they are expensive to operate. Thermal and plasma coating techniques are characterised of low-bonding strength between the HAP coating and the substrate; delamination and accelerated resorption during service. The delamination and rapid resorption of the coating during service is ascribed to the high processing temperatures involved during processing which lead to the decomposition of HAP. The weakened bonding is attributed to the vast temperature mismatches that exist between HAP and Ti-6Al-4V. Fortunately, cold spray technique retaining all the advantages of thermal/plasma spraying techniques, however they are expensive to operate.[11] Also, CS cannot deposit HAP which is a bio-ceramic and lacks the required plastic deformation during coatings. To overcome the shortcoming presented by the HAP material, research currently makes use of bio-composite where a metal and HAP are mechanically milled together to achieve the union. In composite, the metal gives support to HAP, reduces the mismatching thermal properties that exist between substrate and HAP during coating and induces plasticity such that HAP can be cold sprayed.

Cold spray techniques are expensive to operate. To date, laser assisted deposition techniques are being evaluated for HAP coating. laser cladding, direct metal deposition, laser-engineered net shaping technique, and direct laser melting are being investigated.[12-24] In this study, laser assisted cold spray, an extension of cold deposition, is presented. The basic of the technique and the advantages over other traditional techniques are discussed elsewhere.[11] LACS was first demonstrate by Bray et al., [25] in 2006 at the International Congress of Applications of Laser and Electro-Optics held in the United State of America. According to Lupoi et al., [26] during LACS deposition, a laser is able to heat both the substrate and the powder being deposited to temperatures that range between 30% and 70% of the particle melting point thereby being able to reduce the particle strength therefore allowing the particle to deform and build up the coating upon hitting the surface. To date, Olakanmi et al., [11] and Bray et al., [25] have successfully produce metal coatings using LACS technique. In this study, this technique is evaluated for the deposition of Ti-HAP composite powders.

Composite coatings of Ti-HAP have been produced before with non-laser assisted deposition techniques.[4,5,25,27-28] Laser assisted techniques have been used successfully to deposit bio composites of Ti-HAP.[13,29-30] Unfortunately, to date literature is scant on the results of Ti-HAP coatings deposited by LACS techniques. This study seeks to bridge that gap. The LACS

produced Ti-HAP coatings were analysed for the microstructure, phase identification, mechanical property and bio-corrosion using Optical microscope, X-ray Diffraction, Vickers's hardness and Metro corrosion machine.

2.0. MATERIALS AND METHODS

Feedstock Powders and Substrate Materials

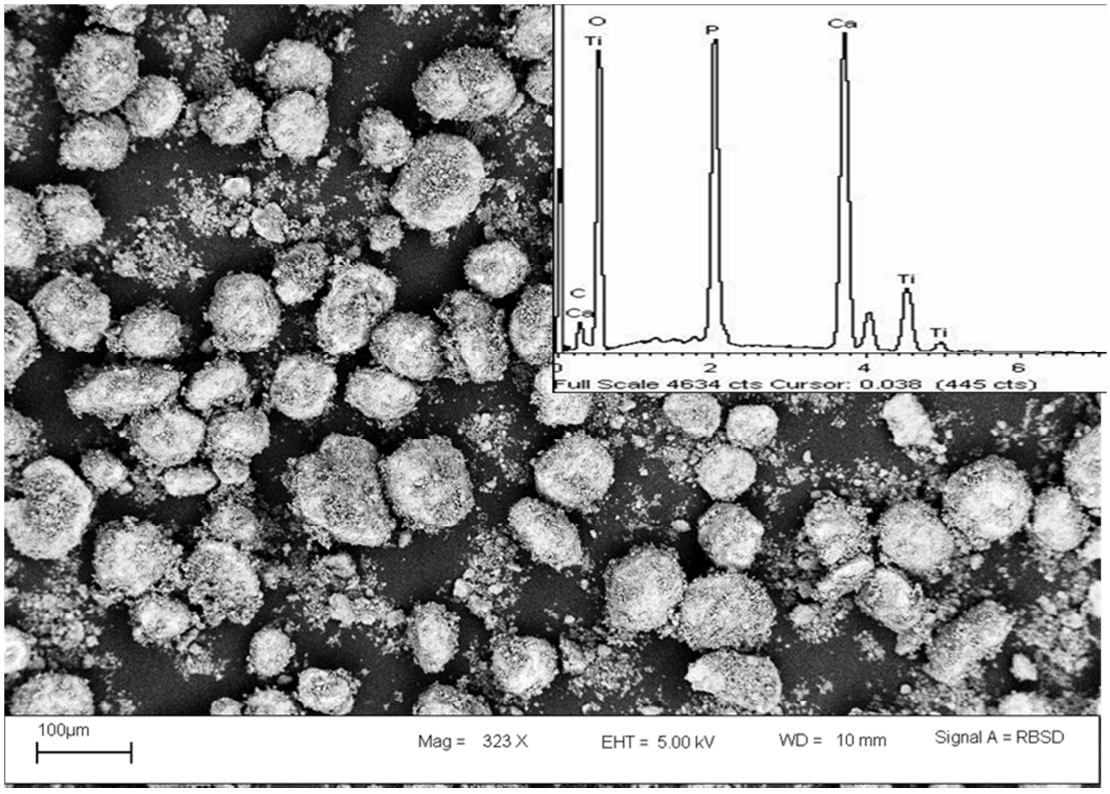

Figure 1: Morphology and composition of the Ti-HAP powders used in this study.

Commercial available pure (CP) spherical titanium (Ti) powder of particle size distribution 45-90 µm supplied by TLS Technik GmbH and HAP (60) of particles size 62.1 µm supplied by Plasma Biotal were subjected to milling using Simoloyer High Energy Ball Mill. The mill used steel balls for grinding process. Figure 1 represents the post milling feedstock that was used to produce the HAP coatings. The powder was tested for flowability using FT4 Powder Rheometer which has 24.5 mm diameter hardened stainless steel blade and 25 mm diameter borosilicate testing vessels. The powder composition analysed with SEM-EDS is shown in Figure 1. Titanium alloy (Ti-6Al-4V) substrates of dimensions 70*70*5 mm^3 were available for use as deposition surfaces. These substrates were initially sand-blasted to improve their

adhesion properties. LACS process requires a well-controlled laser energy output source. In this work, a 4.4 kW 044 Rofin Nd:YAG laser source was used to pre-treat the deposition surface before powder deposition.

2.1. LACS Set-up

The laser-assisted cold spray equipment used in this study was located at the CSIR National Laser (NLC/CSIR), Pretoria, South Africa. The set-up included a 4.4 kW, 044 Rofin Nd:YAG (Rofin DY 044) laser system of 1.06 µm wavelength, a AT-12000HPHV 5000PSI (35 bar) powder feeder (Thermach Inc., Appleton), compressed Nitrogen bulk gas tank with controlled regulation and a de Laval supersonic nozzle. The converging-diverging (de Laval) DLV-180 nozzle used in this study was manufactured and supplied from the Centre for Industrial Photonics, Institute for Manufacturing, University of Cambridge, UK. This nozzle is shown elsewhere.[11] The nozzle was mounted on the Kuka robot arm which allowed for the simultaneous scanning of the laser source spot and the powder spot across the depositing. A well optimised laser-powder spot is characterised by the spot that has the laser spot locking within it the powder spot (See Figure 2). This step allows for the powder to be fully heated and deposit without loss in powder occurring. For the work presented in this study, the powder stream was trailing behind the laser spot by 15 mm with a delayed time of 1.5 seconds.

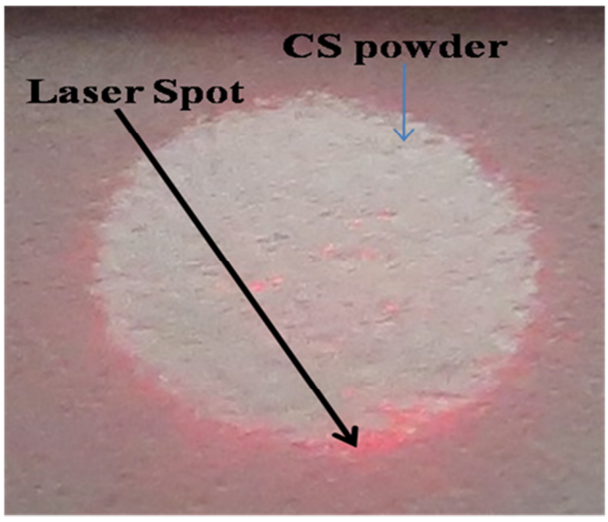

Figure 2: Optimised laser-powder spot interaction.

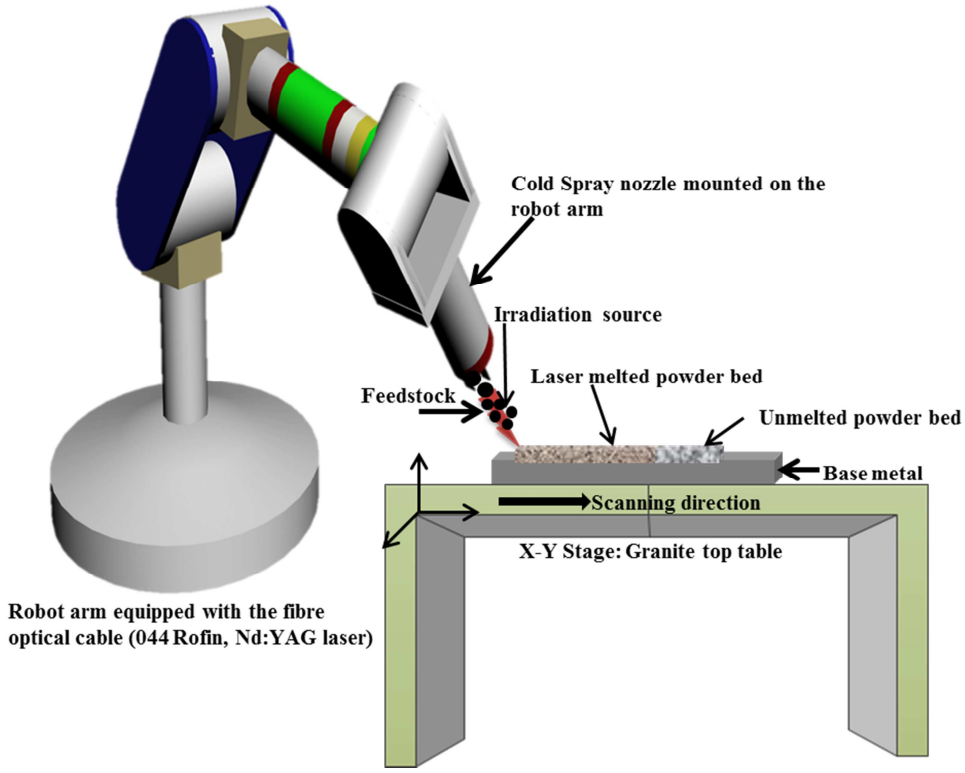

Figure 3: Laser Assisted Cold Spray set-up.

Figure 3 illustrates a typical LACS process set-up. High purity compressed nitrogen gas is desirable. For this work low pressure compression was used were the gas was compressed to 16 bar for the deposition process. In our work, N_2 gas acts as both a carrier and a compressor gas. LACS deposition process requires significant laser power to achieve deposition. The function of laser source was to pretreat the already sand blasted Ti-6Al-4V substrates while softening the substrate before LACS deposition. 2.5 kW laser power was used during process. The nozzle to substrate stand of distance of 50 mm, laser-power spot scanning speed of 30 mm/s and the laser spot inclination of 15° normal to the substrate were used.

2.2. Sample preparation and analysis

The produced coatings were sectioned then ground and polished to a 0.04 micron (OP-S suspension) surface finish with a Struers TegraForce-5 auto/manual polisher. Post polishing, the selected coatings were analyses for microstructures using light optical microscope connected to the Analysis® software and Joel scanning electron microscope (SEM) Model JSM-6510 scanning electron microscope (SEM) and phase composition using Panalytical XPert PRO PW 3040/60 X-ray diffraction (XRD) with Cu Kα monochromater radiation

source. The hardness of the coatings was conducted using Matsuzawa Seiko Vickers micro-hardness tester model MHT-1. An indenting load of 100 g and a 10 second dwell time was used for each hardness indent action. The selected bio-ceramic coatings were sent for bio-corrosion analysis using Metrohm PGSTAT101.

3.0. Results

3.1. LACS coatings microstructures

LACS technology, as a coating technique, has recently emerged where it is now evident that open literature is scant of microstructure which report either deposited HAP or the composite of Ti-HAP. Given this understanding results reported here were compared with those results produced with thermal and cold spray techniques.

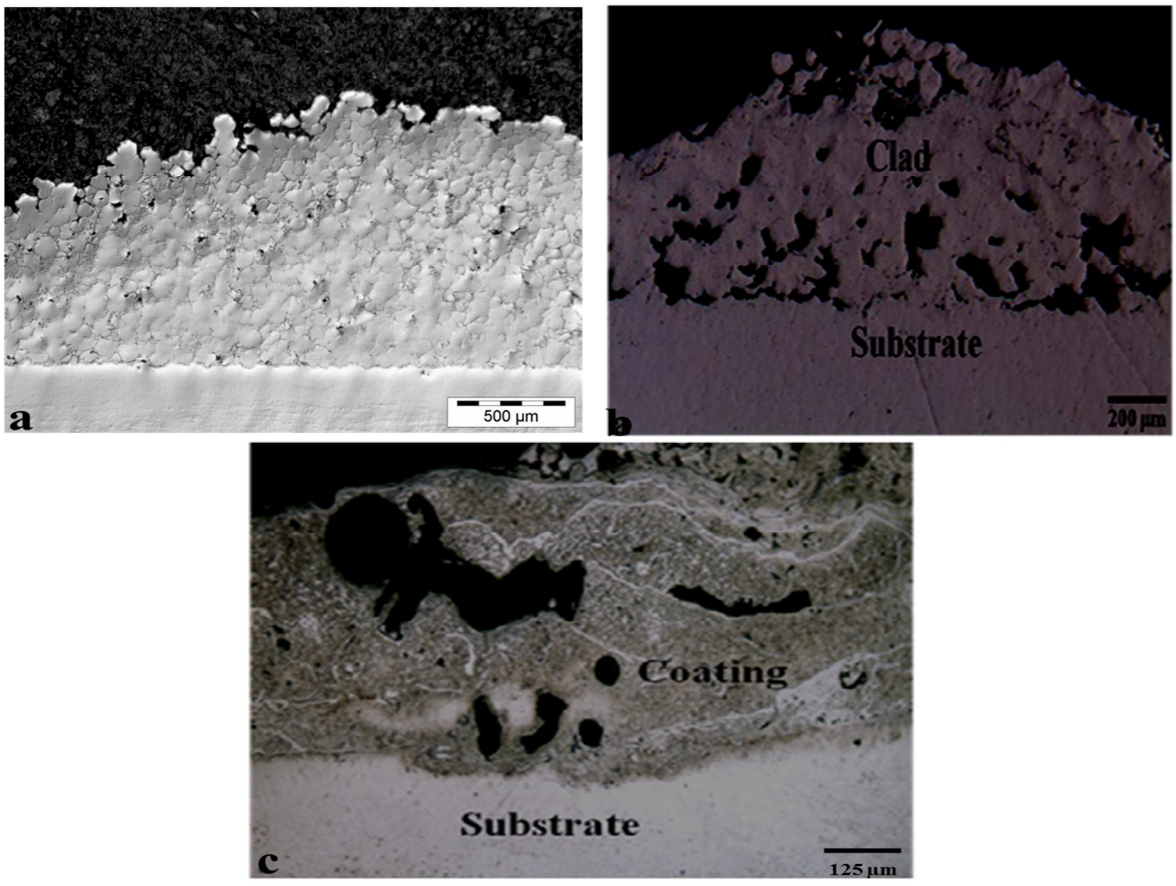

Figure 4: LACS coatings achieved at laser power of 2,5 kW: (a) (CP) Ti powder, (b) 20 wt.%, HAP in composite and (c) 80 wt.%, HAP in composite.

Figure 4 represents LACS coatings of (CP)-Ti, 20 wt. %, HAP and 80 wt. %, HAP in composite powders achieved by laser power of 2.5 kW. Figure 4a presents a well consolidated, pore less, dense coating that is well bonded to the substrate. At this laser power the coating is not affected by oxygen free environment and is not melted. Typically, titanium coatings when affected by processing heat and the open oxygen environment will transform from white (good deposition) to purplish (heat and oxygen affected). Figure 4a details clearly that heat inputs generated were way below the melting point of the titanium powder. Figure 4b represents a coating of powder that had 20% of HAP by mass mixed with 80% (CP)-Ti powder that where milled together. The achieved coating is highly porous, cracked and weakly bonded to the substrate. Figure 4c presents a coating achieved by depositing a powder made of 80% HAP and 20% (CP)-Ti by mass. This coating is porous, crack-free and well bonded to the substrate. In comparison, coatings of (CP)-Ti are porous while the (CP)-Ti coating is pore-free. Good bonding is achieved for (CP)-Ti and 80 wt. %, HAP while the coating made from 20 wt. %, HAP was highly cracked at the interface and therefore was weakly bonded to the substrate. To further investigate the microstructures all the coatings were etched. The optical micrographs of the etched samples are given by Figure 5.

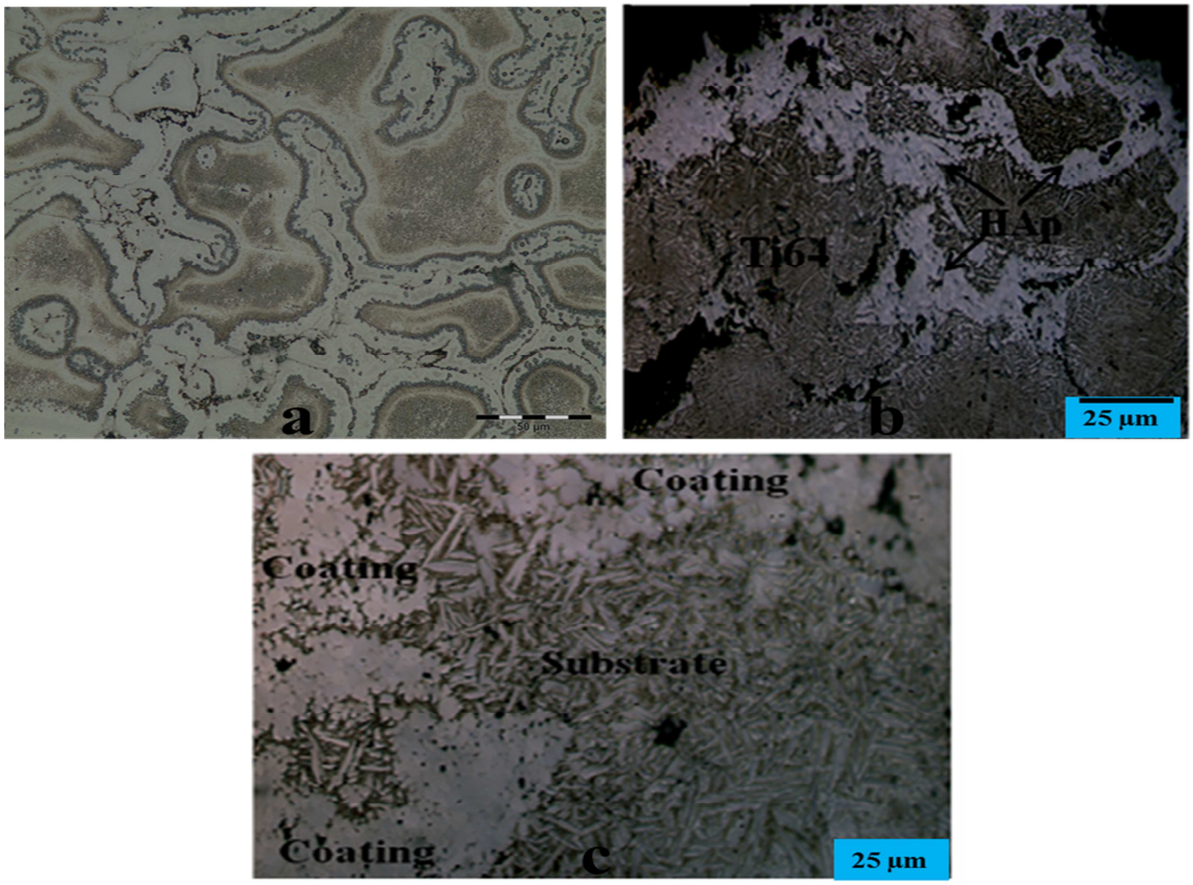

Figure 5: Etched LACS coatings achieved at laser power of 2,5 kW: (a) (CP) Ti powder, (b) 20 wt.%, HAP in composite and (c) 80 wt.%, HAP in composite.

Figures 5a-c represents the etched micrographs of the LACS coatings of (CP)-Ti; 20 wt. %, HAP and 80 wt. %, HAP respectively. Figure 5a reveals the boundaries that represent an island. No pores or unmelted particles are observed at this magnification. The brown colour represents the microstructure of titanium. The coatings represented by Figure 5b is that of the 20 wt. %, HAP. From the cross-section view a white, thick, micro-porous boundary layer of hydroxyapatite can be identified. This white layer that is hydroxyapatite seemingly grows alongside the edges of the coating, the observed cracks and around the pores. It is possible to identify the fine spikes on the coating that are originally from deposited titanium powder. Similar results are reported by Choudhuri et al.,[24] They have attribute the observed microstructure, were HAP grow within the boundaries of Ti, to the encapsulation of HAP particles by the titanium matrix. Figure 5c is a coating that was generated from the 80 wt. %, HAP powder deposited similarly at 2.5 kW laser power. The cross-sectional view reveals that this coating had a thicker, continuous, porous layer of white splats which are from the HAP. It was possible to reveal the spikes of titanium powder which were covered under the HAP

layer. In addition, Choudhuri et al.,[24] concluded that by increasing the HAP content in the powder, the deposition efficiency or the amount of HAP that reports in the coating should increase. This study reports similar observed were HAP layer in the 80wt. %, HAP is most significant that that achieved with the 20wt. %, HAP.

By comparison: It can be inferred that the coatings presented by Figures 5b and c were generated from same heat inputs. This is to say the powders had been heated to the temperatures prior to deposition. To which no melting was achieved. This is said realising that in both coatings, a thick layer of HAP make a cover layer on the substrate not an association/dilution into the substrate. By contrast, the 80 wt. %, HAP coating show spikes of Ti (Figure 5c) which are not easily identified in the 20wt. %, HAP coating (Figure 4b). While the HAP seems to grow on the edges of the coating with the 20wt. %, HAP, it is evident that in the 80 wt. %, HAP coating, HAP make a cover layer on the coating. To ascertain that HAP was present in the 20 wt. %, HAP, this coating was taken for composition and phase analysis using X-ray diffraction, the results are given and discussed in section 3.2 with the hardness tests results of the achieved LACS coatings reported in section 3.3.

3.2. Composition analysis with X-ray diffraction

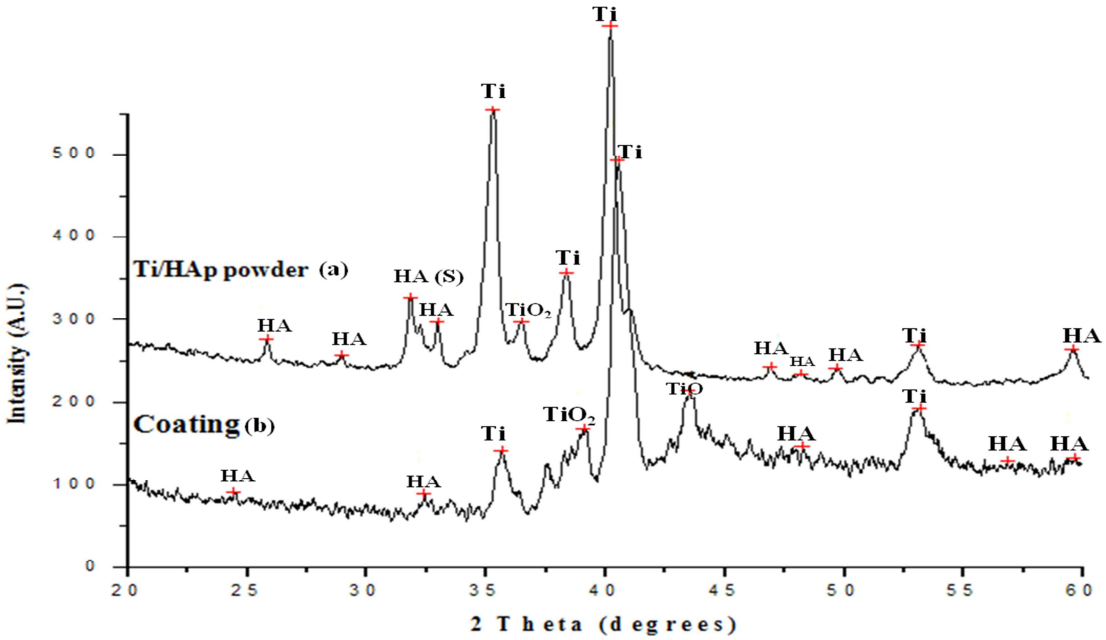

Figure 6: Phase identification by XRD of the 20 wt. %, HAP powder and its LACS coating.

Figure 6 compares 20wt. %, HAP powder (Figure 7a) to its LACS coating (Figure 7b). A similar representation of the phase composition in the two materials is observed. The only difference is the new peak observed at about 43 degrees (TiO) and a shift of the TiO_2 peak from 36 degrees in the powder to 38 degrees in the coating. The peak identification show that the diffraction peak of both Ti and HAP were preserved at exactly 31.77 and 40.170 degrees peak positions respectively. This observation relate to the processing temperatures. Typically, high processing temperatures lead to the decomposition of HAP in coating. In this study, it becomes clear that the chosen laser power and the trailing thereof of powder plum and the laser spot led to low processing temperature which could not altogether destroy the diffraction peak of the HAP in the composite powder. In plasma spraying, HAP decomposition is associated with high processing temperatures and the highly reactive atmospheres. To avoid the occurrence of HAP decomposition, it is proposed that large HAP particles should be coated with a little time interaction between the powder plum and the laser heat. During deposition it was ensured that the scanning time was high given the fast scanning speed over a short area while the powder jet was allowed to trail behind the laser source by several seconds. This could have been the primary reason the HAP was preserved. In addition to the preserved HAP and Ti diffraction peak, TiO and TiO_2 peaks are observed. TiO_2 peak is present in both the powder and the coating. This peak generally indicate an excess oxygen environment, but for this study the powder was milled under a high argon controlled environment which depleted the oxygen while during deposition the process took place in a close chamber. The presence of the TiO_2 peak in both the powder and the coating cement the proneness of Ti to the oxygen which is typically accelerated by increasing the deposition environment temperatures above room temperature. TiO is an indication of low processing temperature and the reduction of TiO2 by Ti in the oxygen depleted environments.

Also to note is the broadening and the dropping in the peak intensity of Ti, TiO_2 and HAP in the coating. These effects are generally associated with the decomposition of HAP in the precursor powder. But, since it is already inferred and deduced from Figure4a that low processing temperatures were achieved during deposition, and that no obvious decomposition phases of HAP are observed, it becomes plausible that in the coating there maybe such phases of HAP which are limited and of low diffraction intensity which makes it difficult to be picked during analysis. This observation is already reported by Zhou et al.[5]

3.3. Hardness profiles

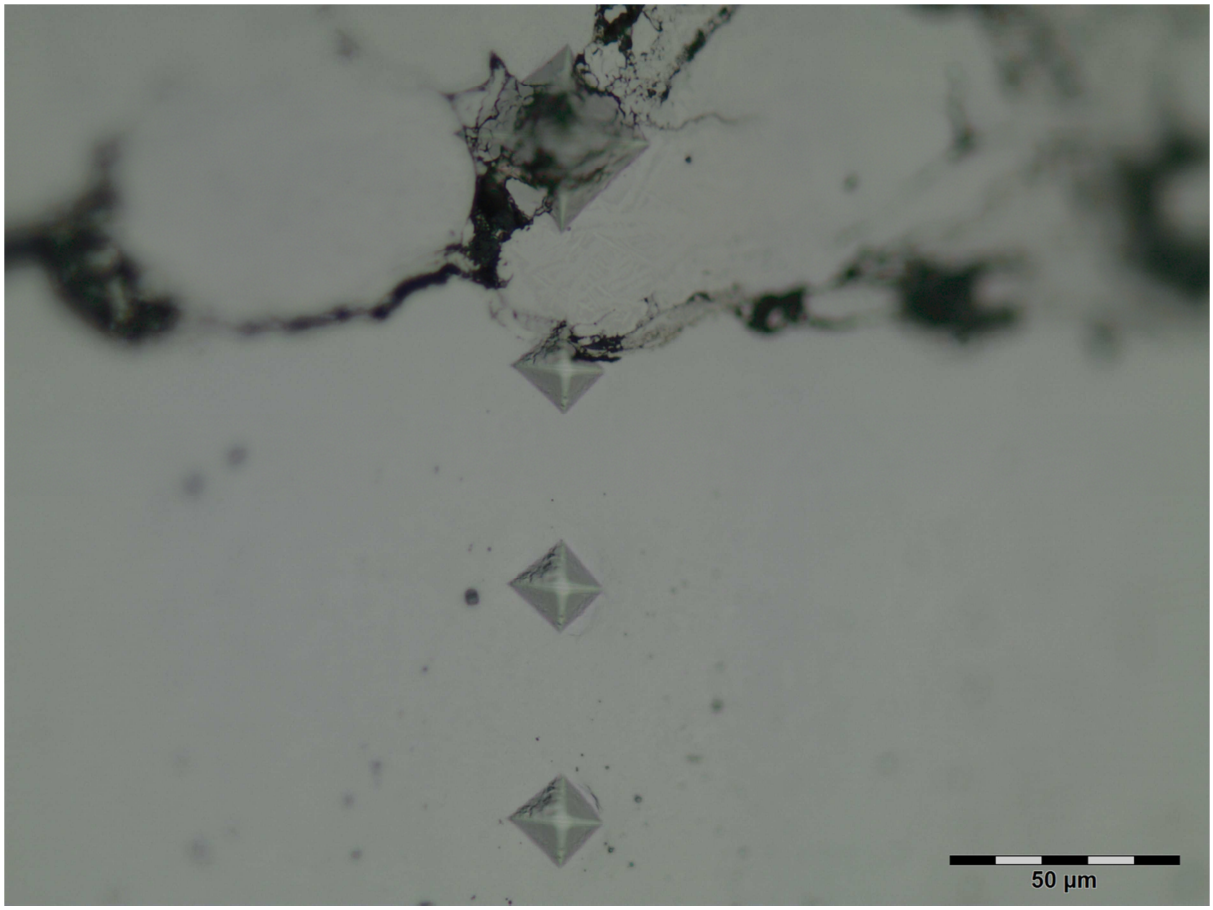

Figure 7: Indentation profile taken across the surface of a LACS coating.

Figure 7 shows the indentation micrograph taken across the surface LACS coating achieved with 2.5 kW laser power. The shown profile reports the hardness indents at the bottom of the coating thereby being able to show the interface point between the substrate and the coating. Typically, the hardness data seek to qualify the mechanical properties of the coatings at the interface. We anticipate that the hardness values will be high at the top of the clad (meaning soft) and will drop considerable across the coating towards the heat affect zone until we reach the natural hardness of the substrate. Also, hardness will be significantly high around the cracks and pores. The hardness profiles of the investigated coatings are given in Figure 8.

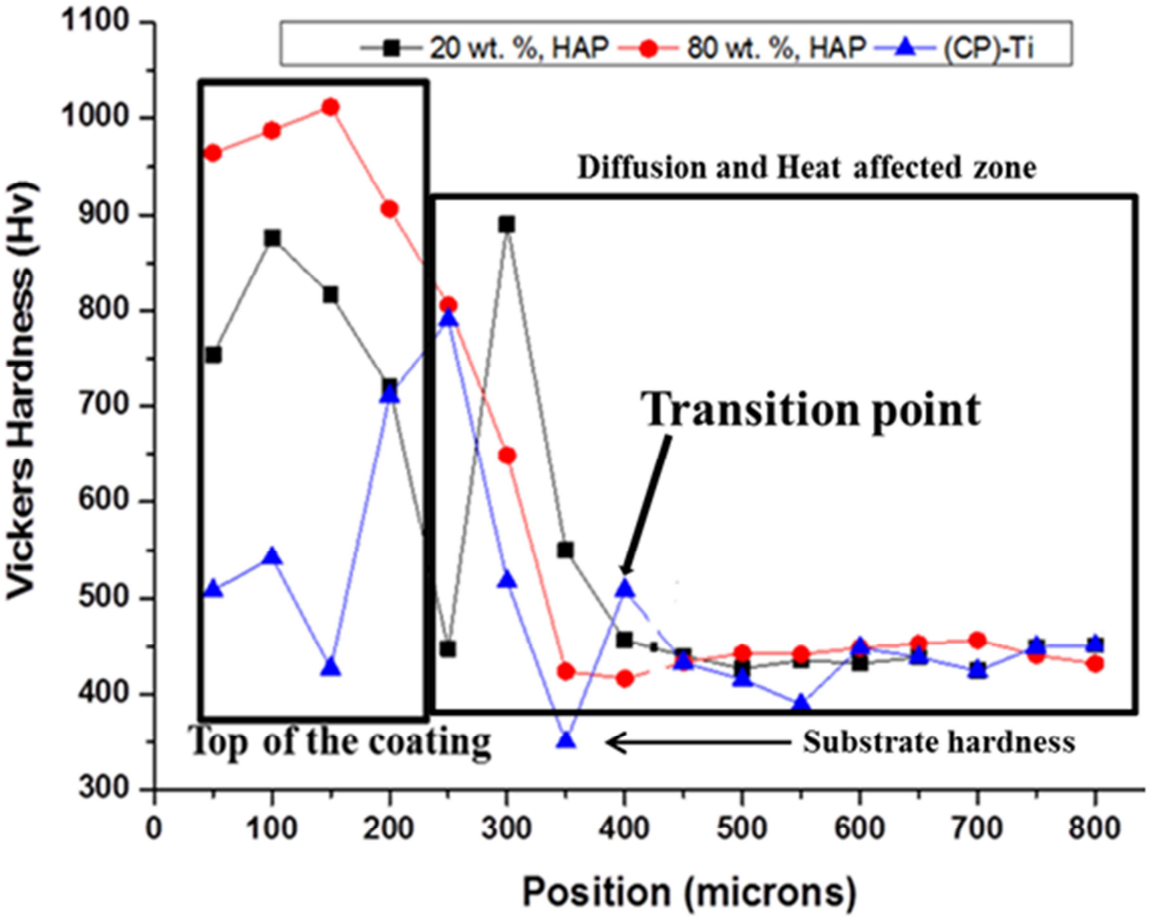

Figure 8: Hardness profile of the LACS coatings.

Figure 8 shows the hardness profiles of the three powders that were deposited at 2.5 kW laser power. Shown in the figure are the diffusion and heat affected zone (HAZ), transition point (TP) and top of the coating (TC). The substrate hardness value as supplied was 355 Hv and can be deduced from the figure as well. It can be deduced from the figure that the clad, which comprised of Ti-HAP (metal-ceramic phases), was hardest followed by the HAZ. The hardness drops significantly across the HAZ towards the substrates. Similar observation has been reported by Mansur et al.[26] The hardness values, now referred to as TP, increased from (CP)-Ti to 20 wt. %, HAP coating to 80 wt. %, HAP coating. This observation could cement the earlier observation which concluded that HAP grew within the Ti matrix in coatings. This is to say the observed drop in the hardness (Hv) values, at the interface, is ascribed to the rapid heating/cooling rates closer to the base metal where the molten Ti particles are able to entrap the HAP particles thereby being able to form the desired metallurgical bonding during cooling.

Choudhuri et al.,[24] reported an adhesion strength of 24. 45 MPa (2. 493 Hv). From the hardness profile it can be deduced that the hardness at the interface were 500, 450 and 400 Hv for CP-Ti, 20% HAP and 80% HAP coatings. The hardness was improved from pure metal to the metal-ceramic coatings. The drop in the hardness from the CP-Ti to 80% HAP at the interface can infer that ceramics made the coating ductile. This ductility is necessary for the medical application in particular for the hip implants/ long bone replacement. Comparing this result to the reported hardness at the interface (TP), it becomes clear that the strength of the ceramics reported here has exceeded those reported for pure cold spraying. In summary, the hardness increases at the top of the coating with increased HAP content, dropped at the HAZ for the ceramic powders, but increased significantly for the metal powder. In a similar fashion, at the transition point, the hardness increases from the metal coating and dropped with an increase in the HAP content. These observations simply conclude that a ceramic-titanium powder has heat resistance properties better than those of pure titanium metal alone. This is true given the individual melting points of the powders: Ti (1660 °C) and HAP (1100 °C). The bio-corrosion tests for the chosen coatings are presented in Figure 9.

4. Bio-corrosion

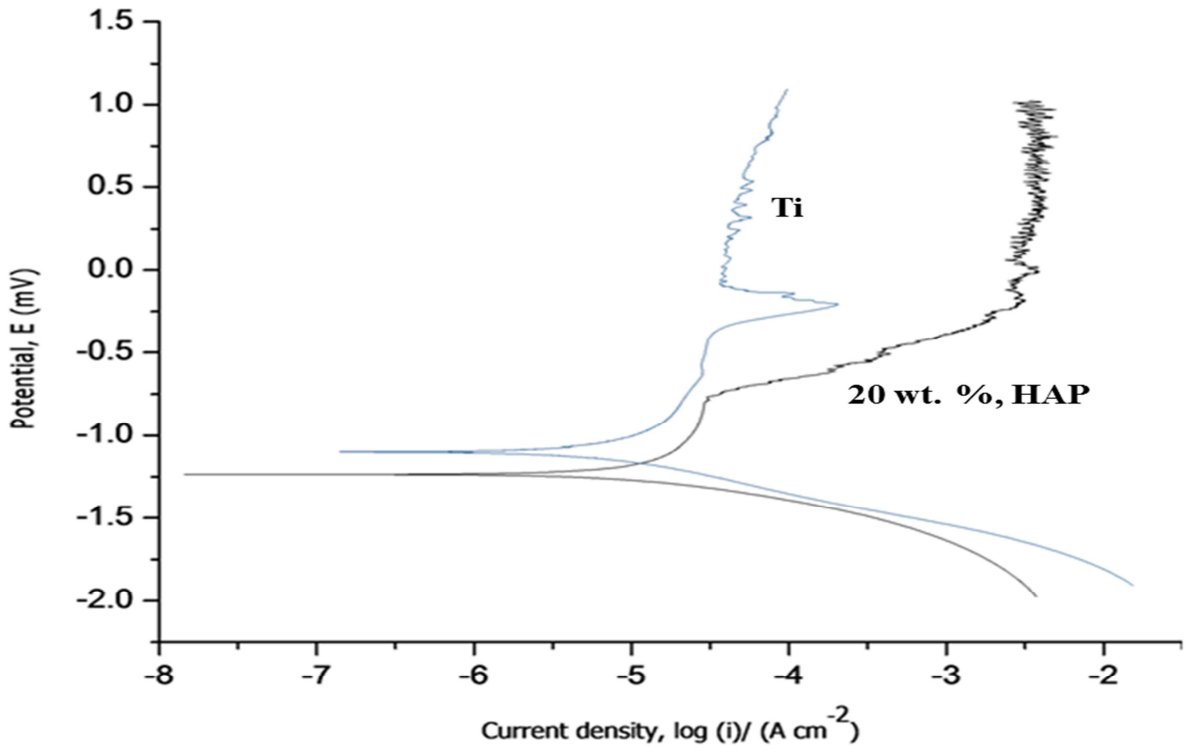

Figure 9: Bio-corrosion of Ti and HAP in Hank's solution.

Figure 9 illustrate the reaction of metal and metal-ceramic coating when they come into contact with Hank's solution. It is known that the inclusion of a ceramic in the composite powder will trigger a continuous activation of the surface which helps strengthen the erosion or the process of metal deposition.[24] From the figure, it can be deduced that in the region -5.5 to about -2.5 A/cm-2 the current was increasing which talks to the kinetic activation of the coating by the Hank's solution. This means, the Ca^{2+} ions from HAP ($Ca_{10}(PO_4)_6(OH)_2$) was reacting well with the simulated body fluid that is Hank's solution. This observation cannot be made with the CP-Ti coating. Also, at the potential value of about 2.5 mV an oscillation in potential is observed for both coating, but it is severe with the CP-Ti coating. This rise and drop in the potential is sometimes due to pitting corrosion taking place. Immediately after the oscillation a passivation layer (region 0.0-5.0 mV) is observed. This is an indication that the corrosion effect was not severe in the coatings where it quickly stabilised in solution. In summary, the ceramic in coating activates the coating to react with the Hank's solution and the presence of titanium provides for the TiO_2 to form where it creates a passivation layer which stabilises the coating in Hank's solution thereby insuring that the coating is not rapidly consumed when in service. From the figure, it was possible to determine the corrosion current and the corrosion potential by the extrapolation method. These values are indicative of the ability for the coating to have pitting corrosion occurring. The values obtained are:

- I_{corr} (Ti) = 5 A/cm^2 and;
- I_{corr} (20 wt. %, HAP) = 4.8 A/cm^2.
- E_{corr} (Ti)= 1.1 V; and
- E_{corr} (20 wt. %, HAP) =1.2V. Similar results were reported by[5, 9].

Similar results have been reported in literature. From these results it can be infer that the 80 wt. %, HAP coating will be more kinetically active in SBF given the thicker HAP layer that was with the optical microscope.

5. Summary

The coatings of (CP)-Ti; 20 wt. %, HAP and 80 wt. %, HAP deposited by laser assisted cold spray technique using 2.5 kW laser power are here presented. The metal coating is characterised of good-bonding, crack and pore-free while cracking and pores where was observed for the 20 wt.%, HAP and 80 wt.%, HAP coatings respectively. It is believed that the observed pores and cracks were filled with HAP which normally break during cold spray deposition given that is brittle. Choudhuri et al., [24] already established that during cold spray deposition, HAP breaks and seek to fill the available voids and cracks. From the etched micro-graphs we were able to establish this observation. It was observed that the HAP coating grew within the titanium matrix of the coating. These results are in agreement with those reported in literature. From Figure 4a, the coating of CP-Ti it was possible to remove altogether the effects of excess heating being generated. Also, it was possible to conclude an oxygen depleted environment. When such condition are met a white coating of titanium is achieved with plasma spraying, otherwise a purplish colour of the coating is seen which indicate that oxidation has took place which generally occurs with excess heat inputs being generated during processing. These deductions were simply corroborated by the XRD diffractogram.

Normally, HAP is prone to excess processing temperature generated from the heat inputs during plasma coating. The general understanding is that when such heat inputs are generated during HAP deposition, the HAP powder will melt and during rapid cooling at the substrate level decomposition occurs. This means when phase analysis is carried out on the coatings, the coatings will have low crystalline phases of HAP. Fortunately, in this work the powder jet was left to trail behind the laser spot, the heat source, by few seconds. This ensured no direct heating of the powder hence in the XRD diffractoram only phases of HAP and Ti were observed. The observed TiO_2 and TiO peaks generally indicate the low processing temperature and the oxygen depleted environment. The broadening and the drop in the intensity of the HAP, Ti and TiO2 peaks in the 20wt. %, HAP coating could mean the feed stock was decomposed, but the decomposed phases of HAP were not observed during phase analysis. This result corroborated those reported by Zhou et al.[5]

The hardness results indicate that all the coatings were well bonded. The coating's hardness dropped from the top of the clad to the heat affected zone. Contrary observation if laser melting and plasma coating's hardness is to be considered. It was observed that the hardness of the coatings increased with an increase in the ceramic content in the powder being deposited. However, it was observed that the hardness at the interface was reversed were the high ceramic content coating, (80 wt. %, HAP), had low hardness. This could be misinterpreted as weak bonding, but it generally speaks to the ductile nature that the ceramic provide to the coating. This ductility is necessary for the bone replacement applications were the metal-ceramic coating will be flexible. Also, this observation can prove that there was an entrapment of the HAP within the titanium matrix. It is explained by Cheng et al., [35] that during heating Ti powder particles are able to entrap the HAP powder which during deposition is able forge the most favourable metallurgical bonding. To it, the same authors using pure cold spray reported a low hardness to the one reported in this study. Meanwhile, the bio-corrosion analysis performed on 20 wt. %, HAP coating and (CP)-Ti showed that the availability of a bio-ceramic in the coating will elevate the kinetics behaviour of the coating when immersed or passed through a simulated body fluids called Hank's solution while the presence of titanium give rise to the formation of an apatite layer which generally creates a passive layer on the coating which then lead to a stable coating which will not degrade fast in service. The similar results can be inferred for the 80wt. %, HAP coating.

6. Conclusion

This study demonstrated that bio-composite powders can be deposited with laser assisted cold spraying. The micrograph indicated that at 2.5 kW titanium powder can be deposited without it being oxidised. In addition the low processing temperature achieved at the selected laser power and rapid scanning speed (30 mm/s), the trailing of the laser spot and the powder jet allow for the minimised interaction time between the powder jet and the heating zone which prevented the powder from decomposing. The XRD results conclude no other phase of HAP being present in the coating. The hardness of the coating was acceptable with low hardness at the interface proving that the HAP was trapped within the Ti matrix hence a ductile layer between the substrate and the coating was achieved. This ductility is necessary for the targeted applications of tissue engineering. In addition, bio-corrosion proved effectively that the presence of a ceramic in the coating will lead it being active in Hank's solution.

Future Work

In future, we wish to establish a fully functional processing window for the deposition of Ti-HAP powder at different levels of HAP in composite. A Taguchi approach will be undertaken. The bio-corrosion test by Metrohm PGSTAT101 machine is acceptable, but it would be good to do soaking test on the coating over a lengthy period of time where the longevity of the coating could be ascertained.

Acknowledgments

The authors wish to give cognisance to the National Research Fund (NRF) and the Council for Scientific and Industrial Research (CSIR) of South Africa for their continued support of funds and resource. While CSIR National Laser Centre is thanked for availing their laboratory equipment that were used for this work. The contribution and insightfulness of Dr. Eyitayo Olakanmi is mostly appreciated while the help of Lucas Mokwena with the experimental setup is generously appreciated. Tebogo Mathebula is thanked for a generosity and willingness to help with material preparation and characterisation is mostly acknowledged.

References

1. R. Geetha, D. Durgalakshmi, and R. Asokamani, *Recent Patents Corr. Sci.* 2, 40 (2010).
2. M.B. Nasab, and M.R. Hassan, *Trends Biomater. Artif. Organs*. 24 (1), 69 (2010).
3. R. Geetha, A.K. Singh, R. Asokamani, and A.K. Gogia, *Progress in Mater. Sci*. 54, 397 (2009).
4. G. Zhao, L. Xia, G. Wen, L.Song, X. Wang, and K. Wu, *Surf. Coat. Technol*. 206, 4711 (2012).
5. X. Zhou, R. Siman, L. Lu, and P. Mohanty, *Surf. Coat. Technol.* 207, 343 (2012).
6. R. Banerjee, S. Nag, and H.L. Fraser, *Mater. Sci. Eng. C.* 25, 282 (2005).
7. S.V. Dorozhkin, *J. Funct. Biomater*. 1, 22 (2012).
8. D. Liu, K. Savino, and M.Z. Yates, *Surf. Coat. Technol*. 205, 3975 (2011).
9. D.G. Wang, C.Z. Chen, J. Ma, and G. Zhang, *Surf. Coat. Technol*. 66, 155 (2008).
10. M. Roy, B.V. Krishna, A. Bandyopadhyay, and S. Bose, *Acta Biomater*. 4, 324 (2008).
11. E.O. Olakanmi, M. Tlotleng, C. Meacock, S. Pityana, M. Doyoyo, *JOM*. 65 (6), 776 (2013).
12. C.S. Chien, T.F. Hong, T.J. Han, T.Y. Kuo, and T.Y. Liao, *Appl. Surf. Sci*. 257, 2387 (2011).
13. S. Nag, S.R. Paital, P. Nandawana, K. Mahdak, Y.H. Ho, H.D. Vora, R. Banerjee, and N.B. Dahotre, *Mater. Sci. Eng. C*. 33, 165 (2013).
14. S.J. Ding, C.P. Ju, and J.H. Lin, *J. Biomed. Mater*. Res. 44 (3), 266 (1999).
15. I-S. Lee, C-N. Chang, H-E. Kim, J-C. Park, J.H. Song, and S-R. Kim, *Mater. Sci. Eng. C.* 22, 15 (2002).
16. D. Wang, C. Chen, J. Ma, and T. Lei, *Appl. Surf. Sci*. 253, 4016 (2007).
17. V. Kokenyesi, I. Popovich, M. Kikineshi, L. Daroczi, D. Beke, Y. Sharkany, and C.S. Hegedus, *Opto-Electro. Adv. Mater. Rapid. Commun*. 1 (4), 171 (2007).
18. S.V. Dorozhkin, *Prog. Biomater*. 1 (1), 1 (2010).
19. R. Sultana, J. Yang, and X. Hu, *J. American. Ceram. Soc.* 95 (4), 1212 (2012).
20. M. Roy, A. Bandyopadhyay and S. Bose, *Surf. Coat. Technol*. 205 (8-9), 2785 (2008).
21. R.A. Ismail, E.T. Salim, and W.K. Hamoudi, *Mater. Sci. Eng. C*. 33 47 (2013).
22. C.S. Chien, T.J. Han, T.F. Hong, T.Y. Kuo, and T.Y. Liao, *Mater. Trans*. 50 (12), 2852 (2009).
23. K.A. Gross, and C.C. Berndt Gross, *J. Biomed. Mater. Res.* 39 (4), 580 (1998).
24. A. Choudhuri, P.S. Mohaunty, and J. Karthikeyan, *Thermal Spraying*, 391 (2009).

25. M. Bray, A. Cockburn, and W. O'Neill, *Surf. Coat. Technol.* 203, 2851 (2009).
26. R. Lupoi, M. Sparkes, A. Cockburn, and W. O'Neille, *Matr. Let.* 65, 3205 (2011).
27. X. Zhou and P. Mohanty, *Electrochimita Acta*, 65, 134 (2012).
28. S-H. Wang, W-J. Shih, W-L. Li, M-H. Hon, and M-C. Wang, *J. Euro. Ceram. Soc.* 25, 3287 (2005).
29. G.J. Cheng, D. Pirzada, M. Cai, P. Mohanty, and A. Bandyopadhyay, *Mater. Sci. Eng. C.* 25, 541 (2005).
30. M.R. Mansur, J. Wang, and C.C. Berndt, *Surf. Coat. Technol.* 232, 482 (2013).